# We are IntechOpen,
# the world's leading publisher of
# Open Access books
# Built by scientists, for scientists

## 6,000
Open access books available

## 148,000
International authors and editors

## 185M
Downloads

Our authors are among the

## 154
Countries delivered to

## TOP 1%
most cited scientists

## 12.2%
Contributors from top 500 universities

CLARIVATE ANALYTICS
**BOOK CITATION INDEX**
INDEXED

**WEB OF SCIENCE**™

Selection of our books indexed in the Book Citation Index
in Web of Science™ Core Collection (BKCI)

## Interested in publishing with us?
## Contact book.department@intechopen.com

**Chapter**

# Electrical Property of Polypropylene Toughened by β Nucleating Agent

*Ling Zhang, Yuanxiang Zhou and Zhaowei Wang*

## Abstract

High-performance polymer insulating material is a crucial knob for developing HVDC power cables. However, the production process of traditional cross-linked polyethylene, especially degassing, is complicated. The space charge accumulation could render severe electric field distortion under high temperatures and electrical stresses, detrimental to the insulation reliability. As a potential alternative, polypropylene (PP) has excellent properties and is environmentally friendly. However, crucial challenges for the PP application include brittleness deficiency at low temperatures and space charge problems caused by toughened PP composites. In recent years, the β nucleating agent (β-NA) has emerged as an effective additive to improve mechanical and electrical properties due to the introduction of the β-crystal form. Herein, PP/β-NA with different contents and self-assembled β-NA were subsequently prepared, respectively. The melting and crystallization behaviors, crystalline structure, and electrical properties were systematically investigated, and the influence on the space charge characteristics of PP/β-NA composites was explored. We aim to summarize the β-crystal form regulation strategies for advanced PP materials and how they perform, point out the critical characteristic parameters to improve the target performance, and offer suggestions for the rational design for future HVDC cable engineering.

**Keywords:** polypropylene, β nucleating agent, crystallization, self-assembly, space charge, electric field distortion

## 1. Introduction

### 1.1 Research background

The transmission line, as the carrier of electric energy, is an essential foundation for the development and progress of the whole power grid. DC cable transmission is not affected by the weather, and thus, its operation is stable and reliable. Compared with AC cable, DC cable has less power loss and lower maintenance cost, which can meet the demand of large-scale new energy power transmission. Therefore, DC cable transmission technology will become an essential link in building the future

energy channel [1]. Cross-linked polyethylene (XLPE) is the main insulation material commonly used in high-voltage DC power cables. It has excellent heat resistance and mechanical properties. Still, it also exposes many problems that cannot be ignored, such as limited transmission capacity, environmental pollution, and space charge accumulation caused by cross-linked by-products [2–4].

To meet the environmental friendliness of power grid and the development demand of large-capacity DC cable transmission in the future, it is vital to develop high-performance and environment-friendly DC cable insulation materials. Among them, polypropylene (PP), one of the five general plastics, has a broad application prospect due to its excellent heat resistance, insulation, low cost, environmental protection, and economy [5, 6].

The properties of PP are affected by its crystalline state. Different crystallization conditions make PP have five structures: α, β, γ, δ, and quasi-hexagonal. Compared with α-crystalline PP, β-crystalline PP has become a research hotspot in recent years because of its loose internal structure and better absorption of external impact.

β nucleating agent (β-NA) was widely used to control the crystalline state of polypropylene so as to obtain an ideal crystalline morphology [6]. The addition of β-NA has little effect on the chemical structure and other properties of PP, so β-NA modification is one of the effective methods to improve its processing and mechanical properties. β-NA plays the role of crystal nucleus, changing the crystalline state of PP and improving its physical properties. However, the β-NA content directly affects the formation of β-crystals in PP materials, and different types of β-NA have different optimal induction amounts.

## 1.2 Space charge of PP materials

In recent years, many scholars have actively explored the electrical properties of PP and its composites [7]. Such as nanoparticle filling, molecular linkage, etc.

Reference [8] found that there were a lot of shallow traps in α-crystalline PP, and the average trap depth in β-crystalline PP was deep. By preparing polypropylene/β-NA DCTH composites, it was found that the increase of β crystal content deepened the average trap depth of the composites and inhibited the accumulation of space charges [9]. It was reported that the β crystal form in block PP introduces deep traps, thus improving the space charge and conductance current characteristics of the material [10].

The use of polymer insulation materials in DC cables will inevitably face the space charge problem, especially when adding elastomer into PP. Many interfaces will be generated, which may aggravate space charge accumulation. In recent years, much research has been carried out on the suppression of space charge in PP materials. The main methods include: 1) nanocomposite; 2) grafting modification; 3) crystal form regulation.

### 1.2.1 Nanocomposite

Deep traps can be introduced into the interface region of nanoparticle-polymer matrix, so nanocomposite is expected to suppress the space charge under DC electric field. As early as 2004, the influence of nanolayered silicate on the space charge characteristics of PP was studied [11] and found that the addition of nanoparticles reduced the accumulation of space charge, and the DC conductivity and breakdown strength of the composites were improved due to the increase of the apparent mobility of carriers. It was reported that the addition of nanoclay made the total space charge of PP nanocomposites higher than that of pure PP [12].

By doping MgO nanoparticles with different contents and surface modification processes in PP, the optimal parameters of space charge suppression were obtained [13, 14]. By doping MgO nanofiller prepared by freeze-drying into iPP/SEBS blends, it was found that when the doping content is only 0.2 wt.%, the injection and accumulation of space charges are well inhabited, and the DC breakdown field strength is increased by more than 10% [15].

Because the relevant theory of nanoparticle-interface effect has not yet been finalized, there is no reliable guiding significance for the selection standard of nanoparticles (such as type, content, particle size), preparation technology of composite, and long-term operation stability, etc. Thus, the macro-scale preparation in engineering is mainly based on experience, and there is a lack of reference operation standard flow.

### 1.2.2 Grafting modification

Compared with nanocomposites, the grafting modification method can effectively avoid agglomeration and make the performance of PP more stable and reliable. As early as 1992, it was found that introducing a small number of polar groups into HDPE can make the space charges in HDPE evenly distributed [16]. After grafting maleic anhydride on the LDPE surface, it was found that the grafted material obviously had less heteropolar space charge accumulation, and the conductance current was significantly reduced [17]. It was also found that the space charge injection amount of PP grafted with maleic anhydride decreased obviously [18]. By measuring the space charge of PP grafted with different content of maleic anhydride at room temperature, the results show that the same polarity charge injection on the cathode side is inhibited after grafting 2% maleic anhydride [19]. In addition, it was found that grafting 1.14% 4-acetoxystyrene into PP can effectively restrain space charge and improve volume resistivity and DC breakdown strength [20].

### 1.2.3 Crystal form regulation

The polymer's crystalline morphology will affect the material's trap characteristics, thus affecting the carrier transport process. By adding β-NA into PP, it was found that the introduction of β-crystal deepened the trap energy level of the composites, thus inhibiting the accumulation of space charges [21]. It is found that when the β-NA doping content is 0.1 wt.% ~ 0.5 wt.%, the composite has a "flower-shaped" β-crystal morphology, and its mechanical properties and space charge suppression effect are the best [22].

## 1.3 Key issues in this research field

DC cable transmission technology will become an important link in building the future energy Internet channel. The development of environmental protection DC cable insulation materials with excellent comprehensive performance is the critical research direction. At present, there are the following problems in the research of PP-based DC cable insulation material modification:

1. The mechanism of β-NA effectively inducing PP to form β-crystal still needs further study. From the influencing factors, the content and morphology of β-NA greatly influence the nucleation effect of β-NA in PP.

2. From the research content, it is mainly concentrated in a single condition, without considering the actual working conditions, that is, different temperature fields and DC electric fields. It is necessary to conduct in-depth research to obtain the optimal modification methods and parameters.

3. Nanocomposite method is not yet mature, so applying it in large-scale engineering is challenging. However, β-NA is used to control the crystal form of PP, and the process is simple and practical, which provides researchers with a new idea of modification.

## 2. Effect of β-NA content on the electrical properties of PP

### 2.1 Microstructure observation

The addition of β-NA will change the crystalline state of polymer materials. Its crystalline behavior, including the changes in cell size and grain size, will also affect the electrical properties of polymer materials. The crystalline materials were observed by polarized light microscopy (POM) to find the relationship between the microscopic crystalline state and the macroscopic characteristics.

Isotactic polypropylene (iPP) was selected as the research object, and the product of Maoming Company of Sinopec (K8003) had a melting point of 162°C, a density of 0.91 g/cm$^3$, and a melting index of 2.5 g/10 min. β-NA is aromatic amide β-NA provided by Shanxi Institute of Chemical Industry. TMB-5 is a white powder with a melting point higher than 340°C, high nucleation efficiency, good dispersibility, and stable structure and performance. The mass fraction of β-NA added was 0.05%, 0.1%, 0.2%, 0.5%, and 1.0% in turn.

In the process of β-NA nucleation, it is often accompanied by a change of micromorphology. Combined with the changes in crystallites observed by a polarizing microscope, the mechanism of β-NA affecting the mechanical properties of materials can be explained. In this paper, Zeiss Gemini SEM 500 ultrahigh-resolution field emission scanning electron microscope was used to observe the brittle section of iPP-βx sample. After spraying platinum on the sample surface, the sample was scanned at 10 kV voltage, and the surface was observed at ×2000.

In **Figure 1d**, there are many regional brittle fracture lines on the brittle section of iPP-pure, which are blocky, and the brittle section is highly uneven. The blocky area of the brittle section of the sample with β-NA addition decreased significantly, and the overall brittle fracture caused the brittle section. When the mass fraction of β-NA is increased, such as iPP-β1.0%, the brittle fracture lines increase. This is also consistent with the phenomenon in the actual brittle fracture process. The specimen with β-NA added is more challenging to be brittle fractured by liquid nitrogen, indicating that its low-temperature toughness has improved dramatically. According to **Figure 1b**, it can be found that the iPP-pure sample has large spherulites, and its low-temperature toughness is poor. When it is brittle broken by liquid nitrogen, there are physical, structural defects in the sample, which easily become the weakness of the whole structure. However, β-NA improves the compactness of crystals from the crystal level, strengthens the connection between crystallites, and makes it difficult to bend and break. However, when the mass fraction of β-NA increases, the uniformity of microcrystalline clusters decreases, and the connection between crystallites worsens.
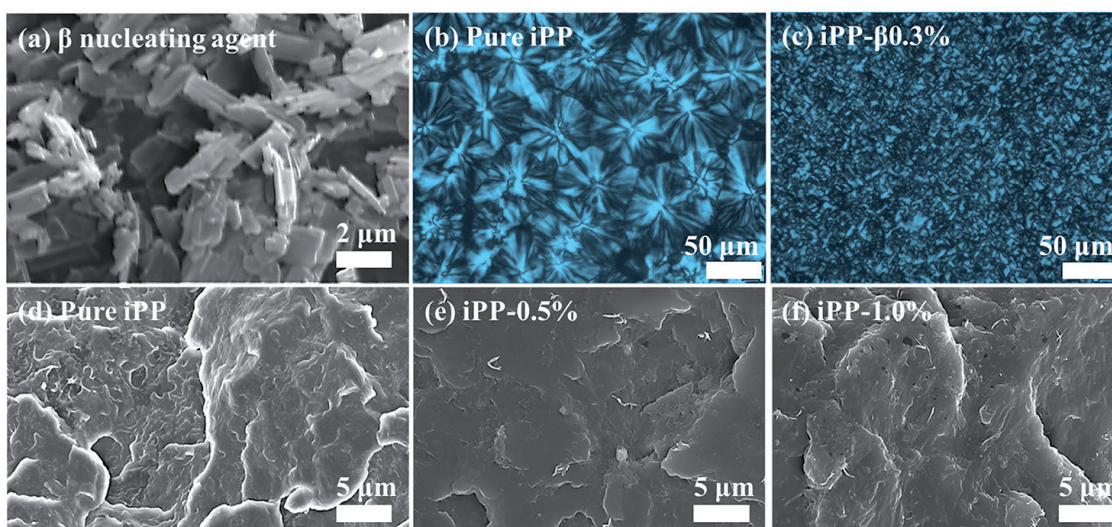
4

**Figure 1.**
*Microscopic observation images of iPP/β-NA sample. (a), (d)-(f) are SEM images, (b) and (c) are POM images.*
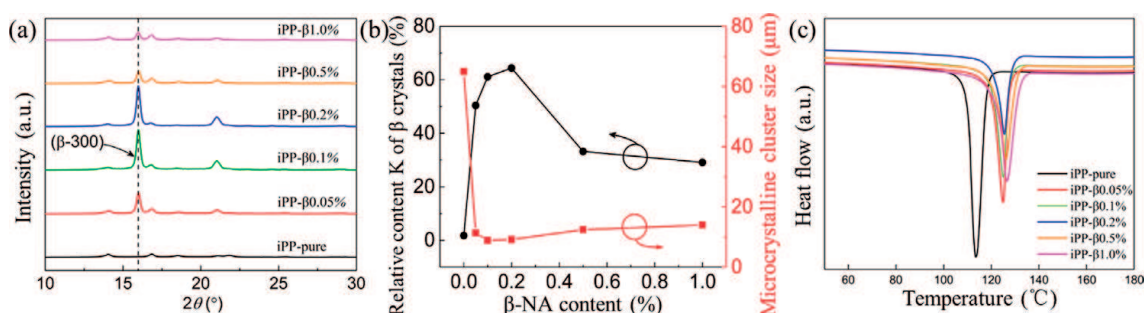


**Figure 2.**
*Crystallization data of β-NA/iPP samples with different contents. (a) XRD spectrum, (b) relative content of β crystal and crystal cluster size, (c) DSC melting curve.*

## 2.2 Crystallization characteristics

iPP is a semicrystalline polymer material, and the nucleating agent controls its crystallization behavior and crystal structure. The change of β-crystal content has the most significant effect on its properties, and the addition of β-NA is one of the most commonly used methods to regulate the crystal form of iPP. X-ray diffraction (XRD) was used to characterize the characteristic peak of the crystal form of the iPP sample, and the crystal composition and relative content of the material were analyzed. The crystal test results are shown in **Figure 2**.

It can be seen from **Figure 2a** that all six groups of samples show typical iPP diffraction patterns [23]. There are both α-and β-crystals in iPP-pure, and the latter is less. In iPP-βx, β crystal is the main component, and a small amount of α crystal is also contained. Combined with the POM observation results of microcrystalline cluster morphology, it was found that β-NA can effectively induce the production of β-crystalline iPP. The β crystal content $K$ of iPP sample is shown in **Figure 2b**. With the increase of β-NA content, the value of $K$ first increases and then decreases. This is because when the content of β-NA in iPP matrix is too high, the dispersion effect becomes worse and local clusters appear, and the total specific surface area of nucleating agent of clusters decreases, which inhibits the process of iPP epiphytic crystallization and heterogeneous nucleation, and the content of β-crystal drops.

The melting behavior of iPP with different content of β-NA was analyzed by a TA Discovery DSC250 differential scanning calorimeter (DSC), as shown in **Figure 2c**. Compared with iPP-pure, the crystallization peak temperature $T_p$ and the initial crystallization temperature $T_0$ of iPP-βx both move toward high temperature, which indicates that β-NA, as an external phase, makes iPP undergo heterogeneous nucleation, which reduces the interfacial free energy of the crystal, thus lowering the nucleation activation energy, and makes iPP form a stable crystal nucleus at a lower supercooling degree, and can crystallize smoothly at a higher temperature. With the increase of β-NA mass fraction, $T_p$ tends to increase, which is more prominent.

## 2.3 Dielectric properties

The dielectric properties of iPP/β-NA composites were tested by a Novocontrol Concept 80 broadband dielectric spectrometer. As shown in **Figure 3a**, compared with iPP-pure, the β nucleating agent of iPP-β0.05% is only 0.05%, while the β crystal content is as high as 50%. The relative dielectric constant has no noticeable change, indicating that the β crystal content has little influence on the relative dielectric constant of iPP materials. TMB-5 β-NA belongs to substituted aryl heterocyclic phosphate, and it also contains impurities consisting of elements P, Na, and Cl, and its polarity is significant [24, 25]. It can be inferred that the relative dielectric constant of
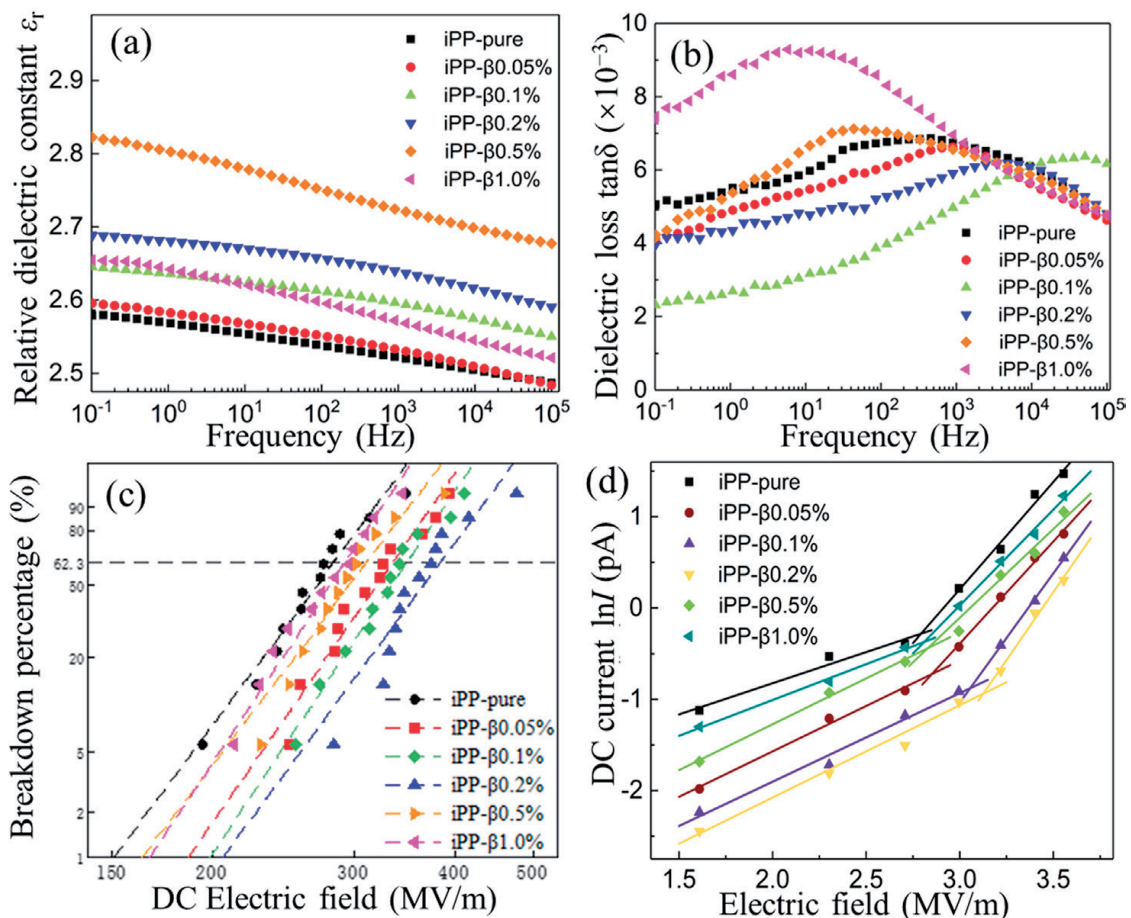


**Figure 3.**
*Electrical properties of β-NA/iPP samples with different contents. (a) Relative dielectric constant, (b) dielectric loss tangent, (c) DC breakdown field strength, and (d) conductance current curve.*

iPP composites is related to impurities, the content of β-NA itself, and its dispersion in the matrix. The more the β-NA content is and the more it is uniformly dispersed, the greater the relative dielectric constant is. When the content of the nucleating agent increases, the polarization of the nucleating agent itself and impurities in the electric field will be enhanced, but excessive β-NA content will also increase the viscosity of the composite system and the movement of its chain segments will be restrained. Overall, the relative dielectric constant increases first and then decreases.

**Figure 3b** shows that when the voltage frequency is lower than 1000 Hz, compared with iPP-pure, the nucleating agent of iPP-β0.05% has a negligible effect, the content of β crystal increases to 50%, and its dielectric loss tangent decreases to some extent. With the further increase of its filling fraction, the dielectric loss tangent decreases at first. It then increases, which indicates that the dielectric loss tangent is also related to impurities, the filling amount of the nucleating agent, and its dispersion. On the whole, the increase of β crystal content is beneficial in reducing its dielectric loss tangent.

DC breakdown strength is an important index to measure the insulation performance of materials. Many accidents often come from the decrease in breakdown strength of insulation materials after the long-term operation of equipment. The distribution of DC breakdown field strength obtained in this paper is shown in **Figure 3c**. With the increase of β-NA mass fraction, the scale parameters of the sample first increase and then decrease, which is consistent with the change of β crystal content in the sample. However, the shape parameters gradually increase, which is related to the crystal's poor uniformity and grain distribution dispersion with the increase of β-NA content.

Compared with breakdown and dielectric properties, direct current conduction can directly reflect the carrier transport process in the material under the action of electric field. To study the change of conductance current of iPP/β-NA composites. **Figure 3d** shows that the conductance currents of six groups of samples are arranged in the following order: iPP-pure > iPP-β1.0% > iPP-β0.5% > iPP-β0.05% > iPP-β0.1% > iPP-β0.2%. As mentioned above, the transition electric field intensity of space charge limiting current, the corresponding turning point voltage is $U_\Omega$, and its corresponding electric field intensity is the electrical aging threshold of the material, which is the initial electric field intensity of the material aging. It is obtained by fitting the turning point of the curve with discrete points in the figure. Overall, β-NA increases the electrical aging threshold of iPP materials, with 0.2% of iPP-β being the largest.

Space charge limiting current can reflect the trap characteristics inside the material. On the one hand, with the increase of β-NA, the conductance current decreases at first and then increases and satisfies iPP-pure > iPP-$\beta_X$. The charge trapped by the deep trap is more difficult to be trapped, and the carrier mobility $\mu$ is smaller. Therefore, the conductance current decreases with the decrease of carrier mobility, which is consistent with the change rule of dielectric loss tangent at low frequency (1000 Hz).

## 2.4 Space charge characteristics

The kinetic evolution of space charge will significantly influence the internal electric field distribution of the sample, and it can also reflect the change of traps in the sample. In this paper, the space charge distribution and dynamic evolution of iPP with different β-NA content are studied based on space charge test platform.

It can be seen from **Figure 4** that when the temperature rises to 70°C, six groups of samples begin to accumulate positive charges near the cathode. With the increase of polarization time, the positive charge injected from the anode migrates to the cathode, and an apparent positive space charge accumulates near the cathode. The injection rate of space charge in iPP-pure is higher than in other groups. With the increase of β-NA content, the accumulation of space charge in the iPP sample first decreases and then increases.

According to the measurement results of space charge in the polarization process, calculate the distortion rate of electric field intensity, and measure three times in each group. See **Table 1** for the average value of each group. It can be seen that at 25°C and 100 MV/m, the electric field intensity distortion rate of six samples is less than 6%, among which the minimum is 4.1% for iPP-β0.2% and 4.3% for iPP-β0.1%. At 70°C, the maximum distortion rate of iPP-pure electric field intensity is 36.1%, the minimum distortion rate of iPP-β0.1% is 13.2%, and that of iPP-β0.2% is 14.8%, which is within the experimental error range.

Generally speaking, the temperature dramatically influences the space charge performance of iPP samples, and the pure iPP samples will have evident space charge accumulation at 70°C. The addition of β-NA can inhibit the space charge accumulation, especially at 70°C. In addition, the β-NA content is about 0.1 wt% ~ 0.2 wt%, which is the best. Space charge accumulation is closely related to trapping parameters. The average trap depth is an important parameter for studying space charges'
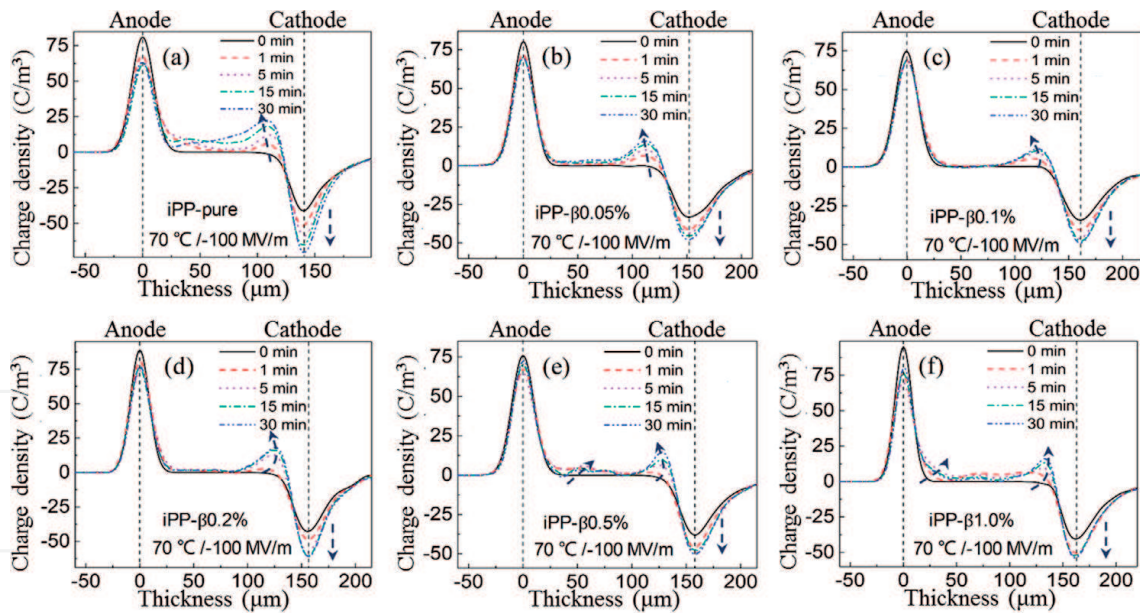


**Figure 4.**
*Space charge distribution of iPP samples at 70°C and − 100 MV/m for 30 min.*

| sample | iPP-pure | iPP-β0.05% | iPP-β0.1% | iPP-β0.2% | iPP-β0.5% | iPP-β1.0% |
|---|---|---|---|---|---|---|
| Distortion rate (%) 25°C | 5.5 | 5.3 | 4.3 | 4.1 | 4.8 | 5.2 |
| Distortion rate (%) 70°C | 36.7 | 25.4 | 13.9 | 14.3 | 21.3 | 28.2 |

**Table 1.**
*Maximum electric field distortion within 30 min under −100 MV/m.*

accumulation and dissipation. Simply put, the larger the amplitude of the average trap depth, the slower the charge dissipation.

## 2.5 Carrier migration characteristics

According to the space charge test results, the variation curve of average trap depth and space charge accumulation is calculated, as shown in **Figure 5a**. With the increase of β-NA content, the accumulated space charge decreases and then increases. The accumulated space charge in iPP-β0.1% is less than that in other groups and iPP-pure > iPP-βx%. The change in average trap depth of the iPP sample is the opposite.

According to the charge injection theory, the charge must overcome a specific barrier $(\varphi_m - \chi)$ to enter the dielectric from the electrode. The difficulty of charge injection increases with the increase of barrier height. Because the electrode materials used in the space charge test are all aluminum, they have the same $\varphi_m$. The electron affinity decreases with the increase of the dielectric constant. Therefore, as shown in **Figure 3a**, with the rise of β-NA mass fraction, the relative dielectric constant of the composite increases first and then decreases, while the electron affinity is on the contrary so that the barrier height increases first and then decreases. Finally, the number of injected electrons Ne decreases first and then increases. It can be seen that the addition of appropriate β-NA is beneficial in inhibiting the accumulation of space charges.

As shown in **Figure 5c**, the contact area between unit cells of microcrystalline clusters in β-crystalline iPP is more significant than that of round α-crystalline iPP, and there are some phenomena such as entanglement of molecular segments, as shown in **Figure 5d**. The current research results show that the electrons in the polymer are easier to pass through the larger free space, including the amorphous region and micropores in the material. The formation of microcrystalline clusters leads to the entanglement of molecular segments, which reduces the free space in the material, makes the electrons more challenging to pass through, and reduces mobility [26].

When the content of β-NA is low, the nucleating agent is uniformly dispersed in iPP matrix, the content of β-crystal gradually increases, the average size of crystallite clusters decreases, the interface area between crystallites increases, and the trap density and average trap depth increase. However, the trap density on the surface of the material is much higher than that inside the material, and the charges injected by the electrode are easily caught by the traps on the surface of the material. The generated internal electric field increases the charge injection barrier of the electrode, and finally, the total charge injection amount decreases [26]. When the β-NA content further increases to 0.5% or even 1.0%, the β-NA particles begin to agglomerate, and the efficiency of β-crystal formation induced by unit mass decreases, which leads to the decrease of β-crystal content, the increase of the average size of crystallite clusters, the reduction of interface area between crystallites, the decline of deep trap density and average trap depth, the weakening of space charge suppression effect, and the rebound of the accumulated amount to some extent.

## 3. Electrical properties of iPP/self-assembled β-NA

### 3.1 Crystallization and morphology observation

From the previous research, it can be found that the nucleation process of TMB-5 β-NA is mainly heterogeneous nucleation. That is, the nucleating agent has alternating
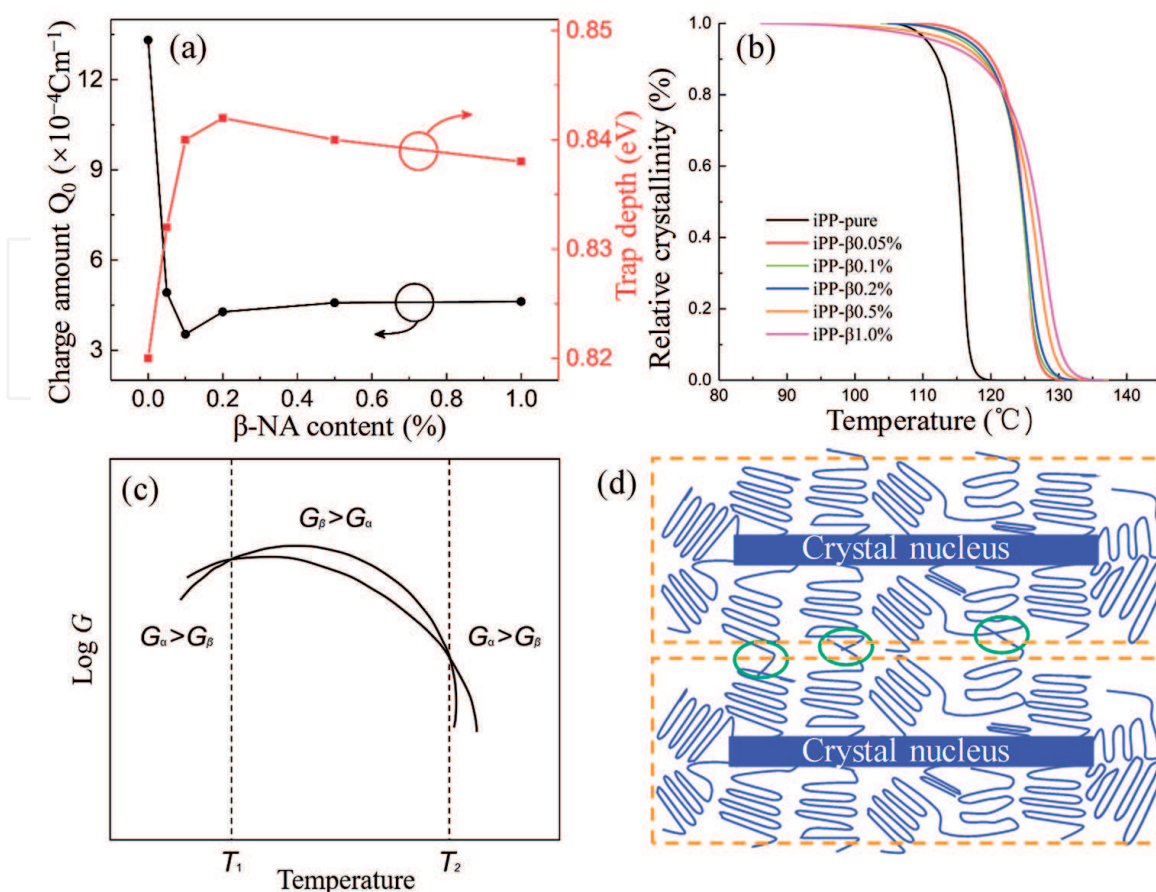
**Figure 5.**
*(a) Curves of space charge accumulation and trap depth and (b) non-isothermal crystallization curves of β-NA/iPP samples with different contents, (c) growth phase diagrams of α-crystal and β-crystal at different temperatures, and (d) schematic diagram of iPP crystallization on β-NA surface.*

polar and nonpolar parts to form a sandwich structure, which contains the molecular chains of iPP and arranges them neatly. The induction effect of the nucleating agent is not only related to its mass fraction but also closely related to its morphology. β-NA can self-assemble into different forms at different hot processing temperatures and has other crystallization regulation behaviors on PP, thus affecting its comprehensive properties [27, 28].

Samples with hot working temperatures of 180°C, 240°C, and 280°C were named iPP-β180, iPP-β240, and iPP-β280, and the control group was iPP-pure, that is, samples without a nucleating agent.

It can be seen from **Figure 6** that iPP-pure shows a typical large-size spherulite morphology at room temperature. The crystallite cluster morphology in iPP-β180 is rod-shaped, while iPP-β240 has an apparent transverse crystal structure, while iPP-β280 offers a feather-like crystal, and the crystal uniformity decreases. When the temperature rises to 180°C until the iPP matrix melts, no nanoscale nucleating agent particles can be observed in iPP-pure and iPP-β180. Still, the self-assembly of the nucleating agent into needle-like structure appears in iPP-β240, and the dendritic network structure appears in iPP-β280. It can be found that the crystalline morphology of iPP is highly similar to that of a self-assembled nucleating agent. This is because the polarity of TMB-5 β-NA is significant, and its solubility in iPP melt is different at different temperatures. When the hot pressing temperature is 180°C, it is insoluble
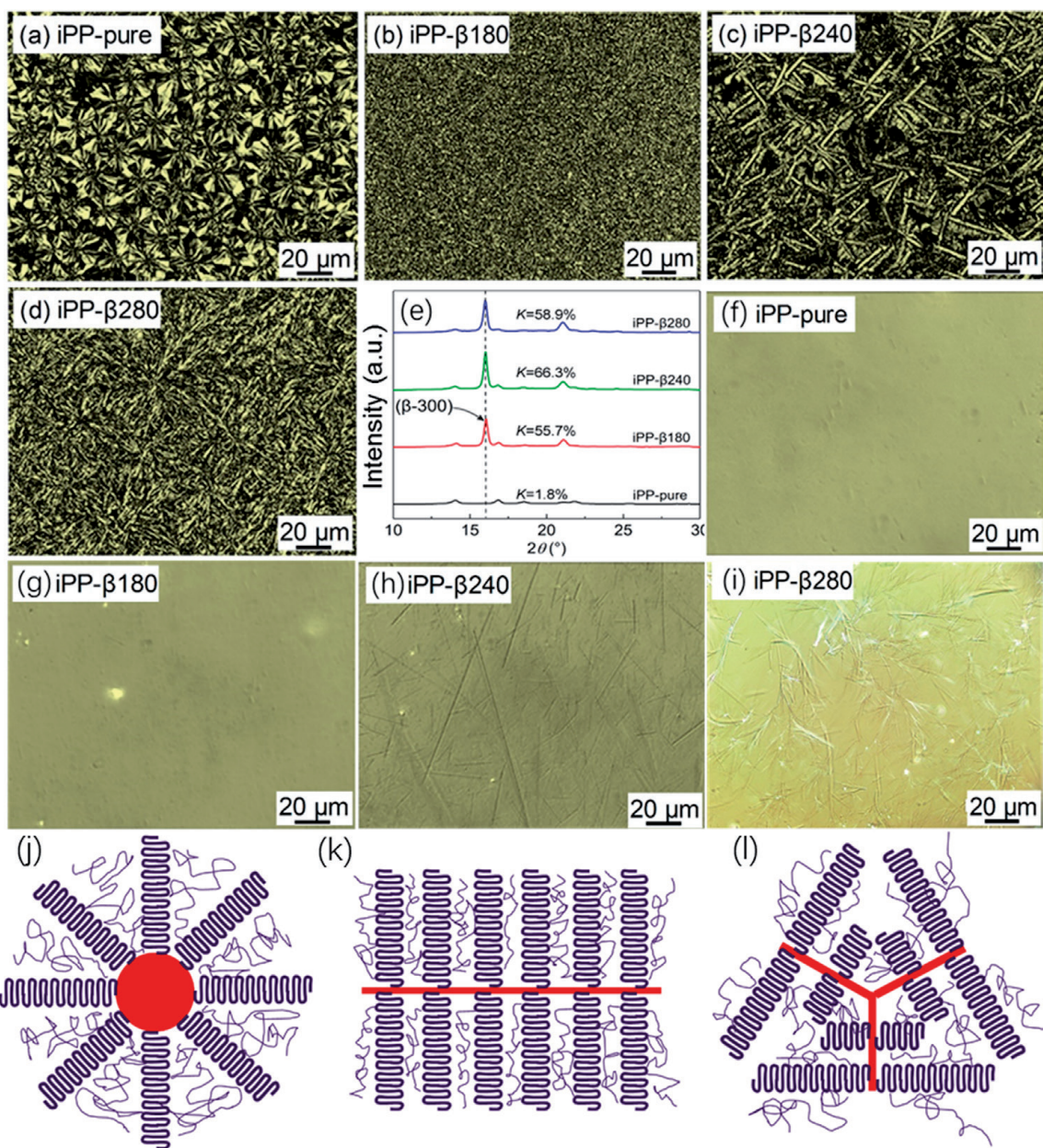
**Figure 6.**
*(a)–(d) POM images of iPP/self-assembled β-NA at room temperature, (e) XRD spectrum, (f)–(i) POM images at 180°C, (j)–(l) schematic diagram of iPP crystal morphology on the surface of self-assembled β-NA.*

in iPP melt and dispersed in iPP in the form of initial particles (nanometer crystals). When the hot pressing temperature rises to 240°C, β-Na dissolves in the molten iPP matrix. In the cooling process, the nucleating agent precipitates first, and the needle-like fiber is self-assembled by intermolecular hydrogen bonding. However, when the processing temperature is further increased to 280°C, the movement ability of the dissolved nucleating agent molecules is enhanced, and the molecules are uniformly dispersed in the matrix. It is easy to precipitate into a dendritic network structure when the temperature is lowered.

The change of self-assembly morphology of β-NA will also make iPP have different crystalline states, and XRD will also test the crystal structure. The XRD test results of iPP/self-assembled β-NA samples are analyzed, and the results are shown in **Figure 6e**. There are both α and β crystal forms in iPP-pure, and the latter is less. In

iPP-βy (y refers to hot pressing temperature), β crystal is the main form, and a small amount of α crystal is also contained. Similarly, the β-crystal content K of the iPP sample is calculated. As shown in **Figure 6**, the K in iPP-pure is only 1.8%, while the β-crystal content in iPP-β240 is the highest, with the K value reaching 66.3%.

Compared with iPP-pure, β-NA nanoparticles in iPP-β180 increased the number of heterogeneous nucleation points in the crystallization process of iPP and promoted the formation of β crystals. The nucleating agent particles in iPP-β240 are dissolved in the matrix, which supports its dispersion in iPP. The nucleating agent self-assembles into acicular fibers. Compared with particles, its total specific surface area increases, improving nucleation efficiency. At the same time, with the rise in hot processing temperature, the movement of the iPP molecular chain is enhanced, and it is easier to be adsorbed on the surface of the nucleating agent, which promotes the nucleation process and further increases the content of β crystals. However, for iPP-β280, the nucleating agent self-assembled into a dendritic network structure, and the total specific surface area decreased compared with that of the needle, which eventually led to the decrease of β crystal content to some extent.

Figure (j)–(l) are schematic structural diagrams of self-assembly of β-NA fused in iPP matrix and subsequent crystallization morphology of iPP. At the low processing temperature of 180°C, β-NA cannot be dissolved in the polymer melt, so it keeps its original dot shape to induce iPP to crystallize into spherulites, as shown in **Figure 6j**. With the increase in hot working temperature, such as 240°C, β-NA gradually melts into the polymer. The nucleating agent can self-assemble when cooled into a fiber needle structure with a high aspect ratio through intermolecular hydrogen bond interaction, as shown in **Figure 6k**. The premise of forming the needle-like structure of the fiber is the melting of the nucleating agent. At a higher processing temperature, such as 280°C, more dissolved β-NA participates in the self-assembly process to produce relatively longer fibers, which are connected to form a dendritic network structure, as shown in **Figure 6l**. At this temperature, the iPP matrix melted, and the nucleating agent remained unchanged. Then iPP epitaxially grew along the surface of the fiber needle nucleating agent, forming a mixed cross-crystal morphology with orientation. In the hot pressing process, the fiber needle-like nucleating agents tend to align along the flow direction so that their alignment is transformed into the orientation of polymer sheets through the template mechanism. The nucleating agent with a high aspect ratio fiber needle structure has the best induction effect, further increases the content of β crystal, and significantly improves its electrical properties. However, with the rise of hot working temperature, when the fibers are connected to form a dendritic network structure, lamellae grow on its surface and finally appear as feather-like crystals. Compared with the needle-like structure of fibers, its total specific surface area decreases, which leads to the decrease of the β crystal induction effect.

## 3.2 Dielectric properties

As shown in **Figure 7**, the self-assembly of β-NA has a specific influence on the dielectric properties of the material. With the increase of hot pressing temperature, the relative dielectric constant increases at first and then decreases. In contrast, the change of dielectric loss tangent is the opposite, in which the dielectric loss tangent of iPP-280 is the smallest, which may be related to the self-assembly of the nucleating agent into a dendritic network structure.
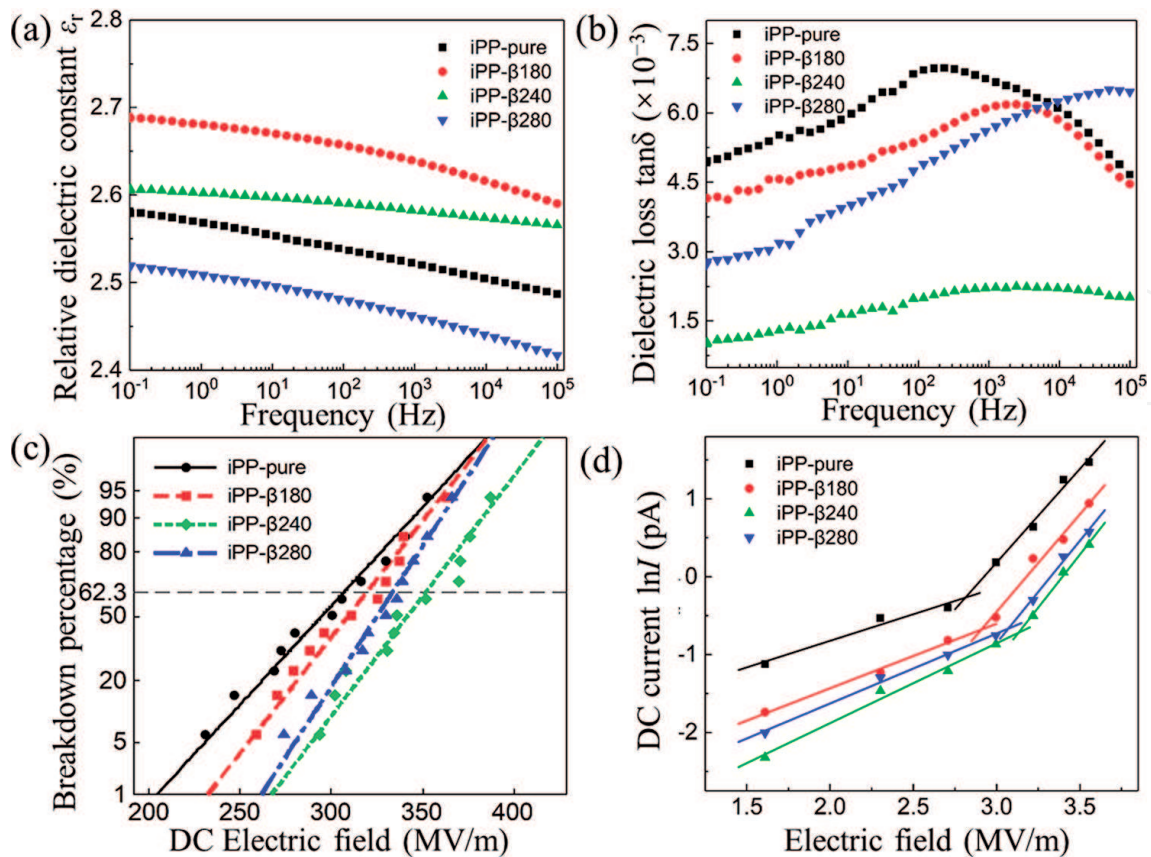
**Figure 7.**
*iPP/self-assembled β-NA sample (a) relative dielectric constant, (b) dielectric loss tangent, (c) DC breakdown field, and (d) conductance current curve.*

It can be seen from **Figure 7c** that the shape parameter of the sample (the dispersion of DC breakdown electric field strength) increases, which indicates that the self-assembly of the nucleating agent makes the uniformity of the sample crystallization decrease to some extent. Under the same external conditions, the DC breakdown electric field strength of the iPP-β240 sample (nucleating agent self-assembled into fiber needle) is the highest, 14.3% higher than that of iPP-pure. However, the DC breakdown electric field strength of iPP-280 decreased to some extent, which was related to the decrease of β crystal-induced generation rate per unit surface area of nucleating agent. At the same time, compared with the test results of DC conductivity current, it was also found that the self-assembled dendritic nucleating agent made the conductivity current of the composite material increase. That is, under the same electric field strength, more charges frequently fell in and out, which would release energy and lead to the decrease of breakdown strength.

**Figure 7d** shows the curves of the experimental conductance current and the applied electric field intensity of four groups of iPP samples in double logarithmic coordinates. Under the same external conditions, the conductance currents of the four groups of samples were arranged in the following order: iPP-pure > iPP-β180 > iPP-β280 > iPP-β240. That is, with the increase in processing temperature, the conductance currents decreased at first and then increased. In addition, the threshold electric field intensity iPP-β240 is the largest. Compared with iPP-pure, adding β-NA or self-assembly into acicular fibers increased the relative content of β-crystals in the

sample, and the DC conduction current decreased. However, when β-NA is self-assembled into a dendritic network structure, its conductance current increases to a certain extent, possibly due to the decrease of β-crystal content. At the same time, the nucleating agents of the network structure were connected in the iPP matrix. Under the influence of impurities, they acted as bridges, leading to the increase in dielectric loss.

## 3.3 Space charge characteristics

The space charge distribution and dynamic evolution of iPP/self-assembled β-NA are shown in **Figure 8**. With the test temperature rising to 70°C, a noticeable accumulation of space charges of different polarities appeared near the cathodes of the four groups of samples. The charges injected by the electrodes easily moved to the opposite electrodes. Among them, iPP-pure samples accumulated more positive body charges, and with the extension of polarization time, there was a growing trend. It is calculated that when the polarization time is 30 min, the charge amount reaches 25.0 ($\times 10^4$c/m), while that of iPP-β240 is only 8.3 ($\times 10^4$c/m), which has the least charge accumulation. It can be seen that the self-assembly of β-NA into fiber needles has a noticeable inhibition effect on the space charge accumulation. However, the self-assembled branch network structure is (8.3 ($\times 10^4$c/m)), and the effect is not apparent.



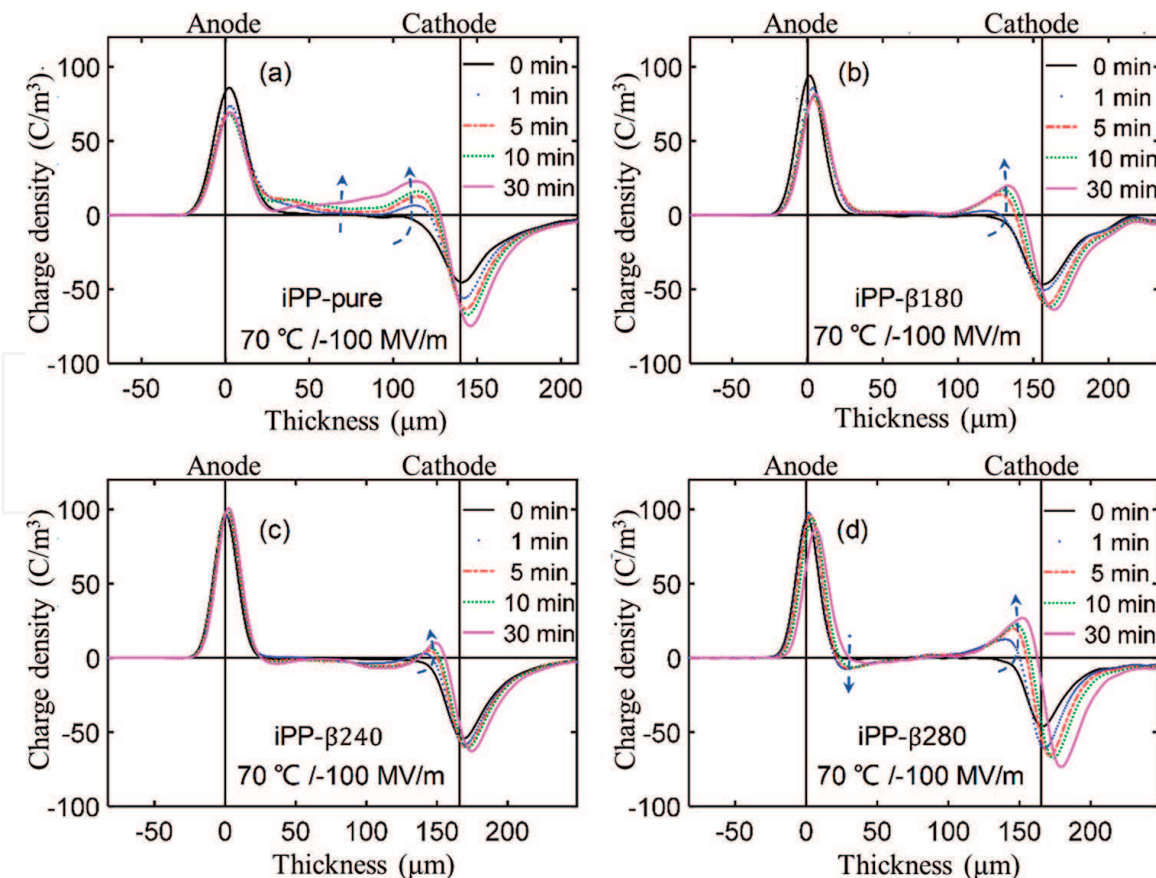**Figure 8.**
*Space charge distribution polarized at 70°C and 100 MV/m for 30 min.*

### 3.4 Electric field distortion

Under the high electric field ($-100$ MV/m), the charge injected into the polymer is trapped by the material trap, accumulating to form space charge, which distorts the electric field intensity in the material, and then generates electrical stress. In severe cases, the internal micropores and cracks will cause partial discharge, and the dielectric will be easily aged for a long time, even breakdown, etc. Therefore, under the same conditions, the distortion rate of the electric field is an important index to measure the space charge characteristics of materials.

As can be seen from **Figure 9a**, the internal electric field intensity of the four groups of samples is distorted to different degrees when polarized at 70°C and $-100$ MV/m for 30 min, and there is a big difference. The distortion of iPP-pure is the most serious, and that of iPP-β240 is better. Among them, the maximum electric field intensity of iPP-pure always rises, while the maximum electric field intensity of iPP-β240 and iPP-β180 remains unchanged after 8 min polarization.

**Figure 9b** shows that the minimum electric field distortion rate of iPP-β240 is only 7.5%, that of iPP-β280 is 31.9%, and that of iPP-pure is 33.6%, which indicates that the addition of β-NA can induce the formation of β-crystal, which can inhibit the space charge accumulation to some extent. However, when β-NA self-assembles into fibrillar needles, the inhibition effect is enhanced, while the self-assembly into the dendritic network is weakened.

On the one hand, the needle-like fiber formed by self-assembly increases the relative dielectric constant of the composite material, and the holes enter the sample through a lower potential barrier so that the injection amount of holes increases. The process of electrons entering the medium from the cathode is the opposite, and finally, the sample as a whole shows the accumulation of positive space charges. At the same time, with the increase in temperature, the excess hole mobility increases and moves to the cathode, and the accumulation phenomenon occurs near the cathode. On the other hand, with the rise of β crystal content in the sample, the average trap depth of the material increases. The surface deep trap traps the charges of the same polarity injected into the electrode, weakening the electric field strength between the electrode and the electrode and inhibiting the further injection of charges. On the contrary, the charges trapped by shallow traps on the material's surface are easy to migrate to the inside, increasing the space charge accumulation. Therefore, the average trap depth of the iPP-β240 sample is the deepest, and its charge accumulation and electric field distortion rate are the smallest.
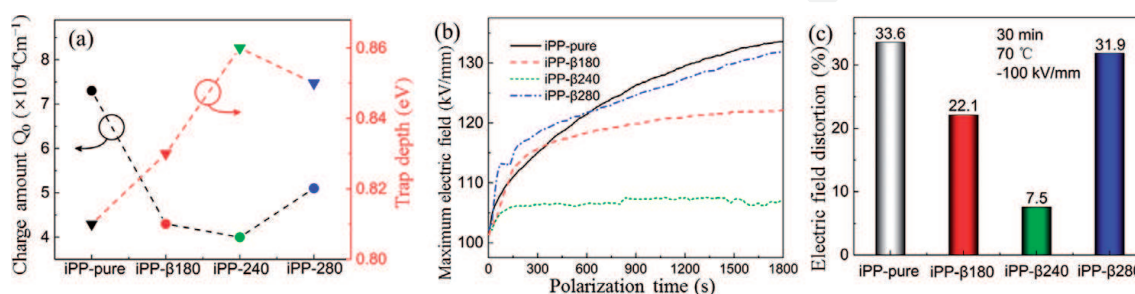


**Figure 9.**
*iPP/self-assembled β-NA samples: (a) space charge accumulation and average trap depth, (b) maximum internal electric field, (c) maximum electric field distortion.*

### 3.5 Trap characteristics

The thermal stimulation current measurement theory (TSC) is developed based on dielectric physics, which can effectively evaluate the microscopic trap parameters of dielectric materials. TSC curve can directly reflect the trap characteristics inside the material. The larger the characteristic peak value, the higher the trap density, and the higher the peak temperature, the deeper the trap energy level. In addition, by secondary calculation of the TSC curve, the corresponding parameters such as trapped charge amount, relaxation time, and activation energy can be obtained.

It can be seen from **Figure 10a** and **b** that the TSC curve of each group of iPP samples is decomposed into two Gauss waves, and the fitting results are all above 0.996. Because each current peak is caused by the release of trap charge, by integrating the current release peak curves of each single trap level, it is found that the trapped charge of the iPP/β-NA sample is more significant than that of Pure iPP. Therefore, β-NA increases the trap trapping ability of iPP composites. This is because, after the introduction of β-NA, more than 90% β crystal form is generated, which brings more interface traps between crystalline and amorphous regions. In addition, β-NA doping increases the activation energy of the carrier relaxation process, thus reducing the relaxation time.
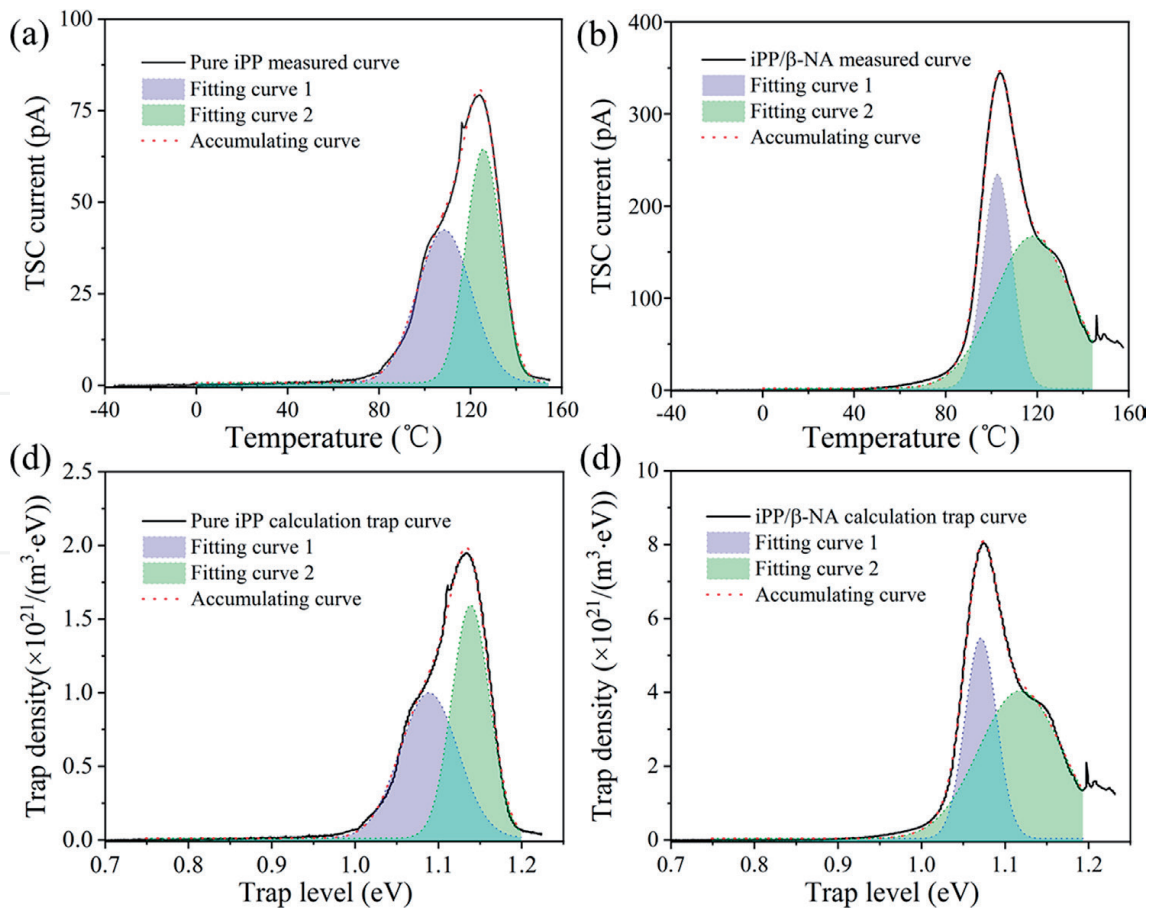


**Figure 10.**
*(a) And (b) TSC current diagrams of iPP materials, (c) and (d) trap energy level density distribution of iPP materials.*

By the improved TSC method mentioned above, the sample's trap level density distribution curves are shown in **Figure 10c** and **d**. The trap energy levels of the two trap peaks of pure iPP are 1.089 eV and 1.138 eV, respectively, and the corresponding trap densities are $1.00 \times 10^{21}/(m^3 \bullet ev)$ and $1.59 \times 10^{21}/(m^3 \bullet ev)$, respectively. At the same time, β-NA doping does not introduce apparent new trap energy levels (shallow traps with trap peaks around 1.1 eV). The addition of β-NA makes iPP lamellae thinner and shorter, and the interface area between the crystalline phase and amorphous phase and physical defects at the interface increase, which also leads to the further growth of shallow trap density [29].

## 4. Conclusion and outlook

### 4.1 Conclusion

iPP/β-NA was used to modify and control different influencing factors, and samples of iPP/β-NA with different contents and iPP/self-assembled β-NA were prepared, respectively. The materials' basic physical and chemical properties and electrical properties were tested and analyzed, and the influence of this modification method on the comprehensive properties of iPP was explored. In this paper, the effects of the content and morphology of β-NA on the space charge characteristics of modified composites under different temperature fields and strong electric field polarization conditions are studied emphatically. According to the processes of space charge injection, transportation, accumulation, and dissipation in different iPP/β-NA composites, the corresponding explanations are given based on the fundamental physical and chemical properties, electrical properties, and related dielectric basis of the composites.

### 4.2 Outlooks

Based on the actual operating conditions of HVDC cables, further research is still needed in the future:

1. The research on the modification of iPP/β-NA can go deep into improving the composites' fundamental properties and space charge characteristics by regulating the non-isothermal crystallization process, including optimizing the cooling rate.

2. In the study of iPP crystal form control to improve the comprehensive properties of composites, the effect of iPP/β-NA/elastomer ternary blend on the crystallization state and comprehensive properties of polyethylene materials can be studied from the point of view of synergy between β-NA and elastomer.

3. Considering the actual operating conditions of DC cables, the test conditions of iPP/β-NA modified composites can be from the actual conditions to the transient conditions such as polarity reversal and pre-breakdown, etc. Meanwhile, the stability of the materials under long-term operation should be emphasized, and the performance comparison with the existing polyethylene-based DC cable materials should be strengthened to study the practicability of iPP-based composites.

## Acknowledgements

## Conflict of interest

The authors declare no conflict of interest.

## Author details

Ling Zhang[1], Yuanxiang Zhou[1]* and Zhaowei Wang[2]

1 State Key Laboratory of Power System Operation and Control, Department of Electrical Engineering, Tsinghua University, Beijing, China

2 Wuwei Electric Power Supply Company of the State Grid, Wuwei, China

*Address all correspondence to: zhou-yx@tsinghua.edu.cn

IntechOpen

## References

[1] Orton H. Power cable technology review. High voltage. Engineering. 2015;**41**(4):1057-1067. (in Chinese). DOI: 10.13336/j.1003-6520.hve.2015.04.001

[2] Maekawa Y, Yamaguchi A, Hara M, et al. Development of XLPE insulated DC cable. Electrical Engineering in Japan. 1994;**114**(8):1-12

[3] Teyssedre G, Laurent C, Montanari GC, et al. From LDPE to XLPE: Investigating the change of electrical properties. Part II. Luminescence. IEEE Transactions on Dielectrics and Electrical Insulation. 2005;**12**(3):447-454. DOI: 10.1109/TDEI.2005.1453449

[4] Montanari GC, Laurent C, Teyssedre G, et al. From LDPE to XLPE: Investigating the change of electrical properties. Part I. space charge, conduction and lifetime. IEEE Transactions on Dielectrics and Electrical Insulation. 2005;**12**(3):438-446. DOI: 10.1109/TDEI.2005.1453448

[5] Hosier IL, Vaughan AS, Swingler SG. An investigation of the potential of polypropylene and its blends for use in recyclable high voltage cable insulation systems. Journal of Materials Science. 2011;**46**(11):4058-4070. DOI: 10.1007/s10853-011-5335-9

[6] Green CD, Vaughan AS, Stevens GC, et al. Thermoplastic cable insulation comprising a blend of isotactic polypropylene and a propylene-ethylene copolymer. IEEE Transactions on Dielectrics & Electrical Insulation. 2015;**22**(2):639-648. DOI: 10.1109/TDEI.2015.7076758

[7] Couderc H, Vanga-Bouanga C, Frechette M, et al. Fabrication and dielectric properties of highly loaded polypropylene micro- and nano-composites. In: IEEE Annual Report - Conference on Electrical Insulation and Dielectric Phenomena, (CEIDP2016); 16-19 October 2016. Toronto, Canada. New York, United States: Institute of Electrical and Electronics Engineers Inc; 2016. pp. 534-537. DOI: 10.1109/CEIDP.2016.7785453

[8] Zhang L, Zhang Y, Zhou Y, et al. Crystalline modification and its effects on dielectric breakdown strength and space charge behavior in isotactic polypropylene. Polymers. 2018;**10**(4):406. DOI: 10.3390/polym10040406

[9] Wu Y, Zha J, Li W, et al. A remarkable suppression on space charge in isotatic polypropylene by inducing the β-crystal formation. Applied Physics Letters. 2015;**107**(11):112901. DOI: 10.1063/1.4930938

[10] Zha J, Yan H, Li W, et al. Morphology and crystalline-phase-dependent electrical insulating properties in tailored polypropylene for HVDC cables. Applied Physics Letters. 2016;**109**(22):222902. DOI: 10.1063/1.4969063

[11] Montanari GC, Fabiani D, Palmieri F, et al. Modification of electrical properties and performance of EVA and PP insulation through nanostructure by organophilic silicates. IEEE Transactio ns on Dielectrics and Electrical Insulation. 2004;**11**(5):754-762. DOI: 10.1109/TDEI.2004.1349780

[12] Fuse N, Ohki Y, Tanaka T. Comparison of nano-structuration effects in polypropylene among four typical dielectric properties. IEEE Transactions on Dielectrics and

Electrical Insulation. 2010;**17**(3):671-677. DOI: 10.1109/TDEI.2010.5492237

[13] Zhou Y, He JL, Hu J, et al. Surface-modified MgO nanoparticle enhances the mechanical and direct-current electrical characteristics of polypropylene/polyolefin elastomer nanodielectrics. Journal of Applied Polymer Science. 2015;**133**(1):42863. DOI: 10.1002/app.42863

[14] Zhou Y, Yuan C, Li CY, et al. Temperature dependent electrical properties of thermoplastic polypropylene nanocomposites for HVDC cable insulation. IEEE Transactions on Diele ctrics and Electrical Insulation. 2019;**26**(5):1596-1604. DOI: 10.1109/TDEI.2019.008198

[15] Zha JW, Wang Y, Wang SJ, et al. Space charge suppression in environmentfriendly PP nanocomposites by employing freeze-dried MgO with foam nanostructure for high-voltage power cable insulation. Applied Physics Letters. 2019;**114**(25):252902. DOI: 10.1063/1.5110443

[16] Yoshifuji N, Niwa T, Takahashi T, et al. Development of the new polymer insulating materials for HVDC cable. IEEE Transactions on Power Delivery. 1992;**7**(3):1053-1059. DOI: 10.1109/61.141811

[17] Lee SH, Park J, Han JH, et al. Space charge and electrical conduction in maleic anhydride-grafted polyethylene. IEEE Transactions on Dielectrics and Electrical Insulation. 1995;**2**(6):1132-1139. DOI: 10.1109/94.484317

[18] Zhou Y, Hu J, Dang B, et al. Mechanism of highly improved electrical properties in polypropylene by chemical modification of grafting maleic anhydride. Journal of Physics D Applied Physics. 2016;**49**(41):415301. DOI: 10.1088/0022-3727/49/41/415301

[19] Zha JW, Wu YH, Wang SJ, et al. Improvement of space charge suppression of polypropylene for potential application in HVDC cables. IEEE Transactions on Dielectrics and Electrical Insulation. 2016;**23**(4):2337-2343. DOI: 10.1109/TDEI.2016.7556511

[20] Liang Y, Liu LZ, Zhang WL, et al. Preparation and electrical properties of 4- acetoxystyrene grafted polypropylene for HVDC cable insulation. Journal of Materials Science Materials in Electronics. 2020;**31**(5):1-9. DOI: 10.1007/s10854-020-02934-6

[21] Zhang L, Teng CY, Zhou YX, et al. Direct correlation between charge evolution and crystalline structure in isotactic polypropylene. In: Proceedings of the IEEE International Conference on Properties and Applications of Dielectric Materials (ICPADM2018); 20-24 May, 2018. Xi'an, China. New York, United States: Institute of Electrical and Electronics Engineers Inc; 2018. pp. 279-282. DOI: 10.1109/ICPADM.2018.8401264

[22] Zhang W, Xu M, Huang KW, et al. Effect of β-crystals on the mechanical and electrical properties of β-nucleated isotactic polypropylene. IEEE Transactions on Dielectrics and Electrical Insulation. 2019;**26**(3):714-721. DOI: 10.1109/TDEI.2019.8726016

[23] Turner-Jones A, Cobbold AJ. The β crystalline form of isotactic polypropylene. Journal of Polymer Science Part B: Polymer Letters. 1968;**6**(8):539-546

[24] Mohmeyer N, Schmidt H, Kristiansen PM, et al. Influence of chemical structure and solubility of Bisamide additives on the nucleation of isotactic polypropylene and the improvement of its Ch arge storage properties. Macromolecules.

2006;**39**(17):5760-5767. DOI: 10.1021/ ma060340q

[25] Nagasawa S, Fujimori A, Masuko T, et al. Crystallisation of polypropylene containing nucleators. Polymer. 2005;**46**(14):5241-5250. DOI: 10.1016/j. polymer.2005.03.099

[26] Jones JP, Llewellyn JP, Lewis TJ. The contribution of field-induced morphological change to the electrical aging and breakdown of polyethylene. IEEE Transactions on Dielectr ics and Electrical Insulation. 2005;**12**(5):951-966. DOI: 10.1109/ TDEI.2005.1522189

[27] Luo F, Geng C, Wang K, et al. New understanding in tuning toughness of β-polypropylene: The role of β-nucleated crystalline morphology. Macromolecules. 2009;**42**(23):9325-9331. DOI: 10.1021/ ma901651f

[28] Varga J. Supermolecular structure of isotactic polypropylene. Journal of Materials Science. 1992;**27**(10):2557-2579

[29] Meunier M, Quirkee N. Molecular modeling of electron trapping in polymer insulators. The Journal of Chemical Physics. 2000;**113**(1):369. DOI: 10.1063/1.481802